Supplementary Information for

Integrative optofluidic microcavity with tubular channels and coupled waveguides via two-photon polymerization

Yonglei Li,[a,b] Yangfu Fang,[a] Jiao Wang,[a,c] Lu Wang,[a]

Shiwei Tang,[a] Chunping Jiang,[b] Lirong Zheng[c] and Yongfeng Mei[a]*

[a]Department of Materials Science & State Key Laboratory of ASIC and Systems, Fudan University, Shanghai 200433, China.

[b]Key Laboratory of Nanodevices and Applications, Suzhou Institute of Nano-tech and Nano-bionics, Chinese Academy of Sciences, Suzhou 215125, China.

[c]School of Information Science & Technology, Fudan University, Shanghai 200433, China.

*Correspondence: Yongfeng Mei (yfm@fudan.edu.cn)

Fiber-based transmission measurement setup

Transmission spectra measurement based on tapered fiber is an effective method to characterize the properties of microcavities which support whispering gallery modes (WGMs). It is based on the overlap and selective phase-coupling of the optical fields between the spindly fiber waist and the resonator's evanescent tail. This method can real-time adjust and optimize the coupling condition to realize efficient coupling.

The whole schematic of this measurement method setup is shown below in Fig. S1. An external-cavity laser Ando 4321D, as the tunable laser source in communication band, was utilized to excite and transmit light though a single-mode fiber (Corning SMF-28e). Part of the fiber had been adiabatically drawn, by a hydrogen torch, to form a thin fiber taper. The taper waist was approximate 1 μm so that light energy would partly leak out from the fiber. Light at certain wavelengths could escape from the waist, overlap and be coupled into the orthogonal tubular microcavity nearby. With a piezoelectric ceramic nanopositioning system (30 nm encoded resolution), the coupling condition could be carefully adjusted by preciously changing the distance between the tapered fiber and the tubular microcavity. After the coupling region, the residual light in the fiber was converted into electrical signals via a photoelectric detector (Thorlabs), displayed in a digital multimeter (Aglient 34401A) and finally collected and monitored by a testing computer. The data acquisition was accomplished through program software LabVIEW and GPIB (General-Purpose Interface Bus) data acquisition card (National Instruments). Through this method, Transmission spectra containing WGM dips for measured microcavities could be displayed in the computer along with the wavelength sweep of the laser source.

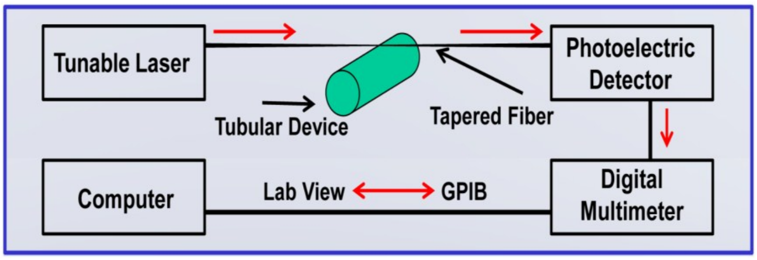

Fig. S1 Schematic of the setup for characterizing tubular microcavities by transmission spectra measurements. This is based on the evanescent field coupling through a tapered fiber. Light at certain wavelengths would escape from the waist of the fiber, couple into the cavity and cause Lorentzian-shaped dips in the transmission spectrum displayed in the final testing computer, which is real-time monitoring the residual light in the fiber through software LabVIEW and GPIB card.

Liquid injection

In our work, liquid sensing measurements were carried out under the liquid-in-tube configuration. This configuration was realized by injecting liquids into one reservoir of the tubular device with a glass capillary under the help of an external microsyringe. First, the capillary was stretched to ensure its end smaller than the reservoir, so that the capillary could be moved and inserted into one reservoir (Fig. S2a) of an empty tubular microcavity (Fig. S2b) with the assistance of a piezoelectric positioning stage. The other end of the capillary was connected to a microsyringe pump. By gradually increasing the injection force, Liquid in the syringe and capillary would be slowly injected into the reservoir and then filled the whole tubular component (Fig. S2c). Equally, liquid could also be drainaged from the tubular structure and the reservoir in the same way. By this means, liquids with various refractive index could be applied and measured sequentially.

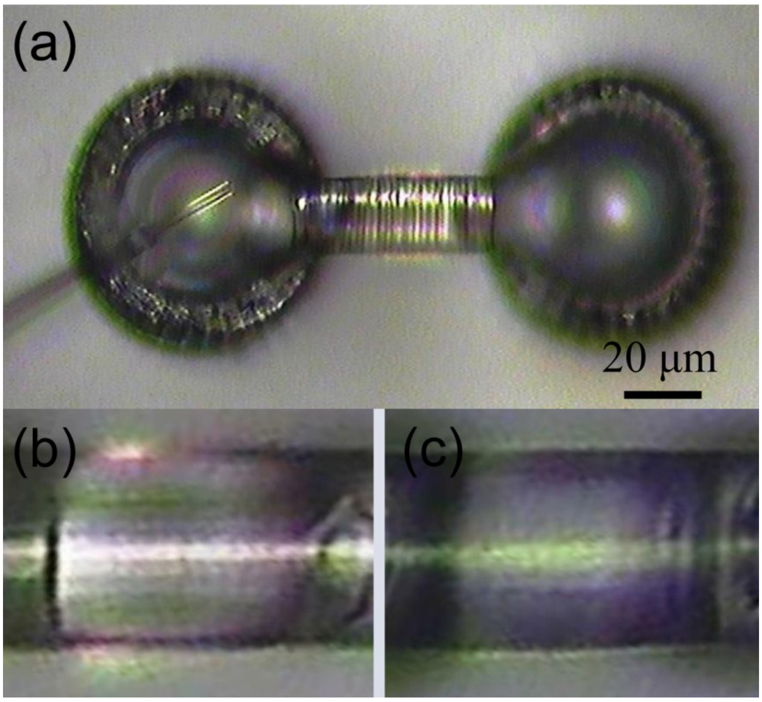

Fig. S2 Realization of liquid-in-tube configuration. (a) Optical microscope image of a stretched capillary inserted into one reservoir of a tubular device in order to inject liquids. The liquid injection situation could be precisely controlled by an external microsyringe and a piezoelectric positioning stage. Enlarged optical microscope photos for a tubular component (b) without liquid and (c) filled with liquid. The two opposite status can be judged by different color contrast.

Parameter verification for fabricated tubular microcavities

After device fabrication, scanning electron microscopy (SEM) was utilized to verify the parameter of the fabricated devices. Microtube diameters have been confirmed by the SEM images in the main paper (Fig. 2 and Fig. 5), but it is inconvenient to clearly observe the wall thickness (cross section) of a horizontal microtube. By virtue of the fabrication principle of direct laser writing, a vertical mircotube, with the same modified parameter setting, was fabricated for the easy detection and verification of wall thickness. Fig. S3 shows the SEM image of a fabricated vertical tubular microcavity (D = 20 μm, T = 0.5 μm). Insert is the enlarged slight-slope view of the tube wall, the yellow scale bar is 0.5μm, and the measured results agree well with the parameters set. This can also verify the fabrication accuracy of direct laser writing.

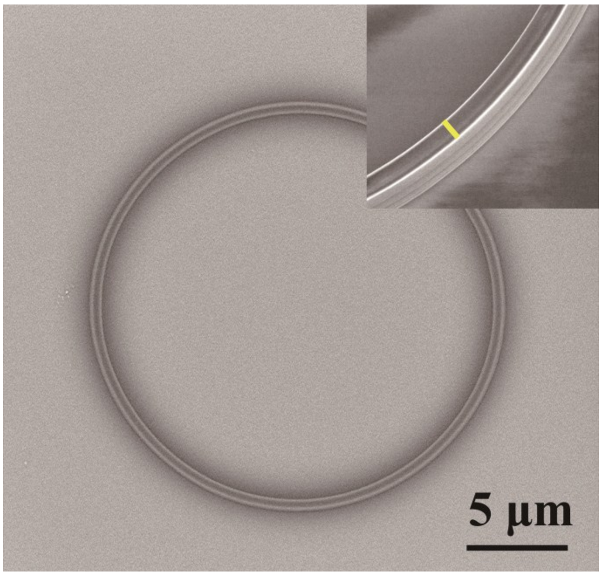

Fig. S3 SEM image of a vertical tubular microcavity (D = 20 μm, T = 0.5 μm). Insert shows the enlarged slight-slope view of the tube wall. The yellow scale bar is 0.5 μm.

Mie scattering theory

The optical properties (whispering gallery modes, WGMs) of tubular microcavities have been studied by a variety of analytic and numerical methods[1-8]. Among them, Mie scattering theory is extensively used because it is easy and fast to implement this theory in multi-layer structures like liquid-in-tube configurations. Besides, based on the solutions to Maxwell's equation in the cylindrical coordinates[3,4], Mie scattering theory is more rigorous and can give more accurate resonant wavelengths and Q-factors for small microtubes[3-5].

For Mie scattering theory, a tubular microcavity can be regarded along the z direction, and the cross section of the microtube can be treated as an N-layered cylindrical structure shown in Fig. S4. The layer indices i of the hollow core and outer background are 1 and N+1, respectively.

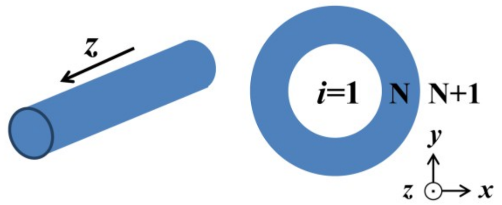

Fig. S4 Schematic diagram of an *N*-layered cylindrical structure (tubular microcavity).

With incident light, transverse-magnetic/transverse-electric (TM/TE) waves can be excited propagating in the *r*-*θ* plane with the electric/magnetic part along the *z* direction. For TM modes, the electric field in the *i*th layer can be expressed as:

$$E_{i,z} = \sum_{-\infty}^{\infty}\left[a_{i,m}J_m(k_ir) + b_{i,m}H_m^{(1)}(k_ir)\right]e^{i\omega\theta}, \tag{S1}$$

where $k_i = n_ik_0$, n_i is the refractive index and k_0 is the wave number in vacuum. The origin of cylindrical coordinates (*r*, *θ*) is at the center of microtube, with Bessel function J_m and Hankel function of the first kind $H_m^{(1)}$ standing for incident and scattering waves, respectively. Using continuities of E_z and $\frac{\partial E_z}{\partial r}$, we have this formula:

$$\frac{J_m'(k_{i+1}r_{i+1}) + D_{i+1,m}H_m^{(1)'}(k_{i+1},r_{i+1})}{J_m(k_{i+1}r_{i+1}) + D_{i+1,m}H_m^{(1)}(k_{i+1},r_{i+1})} = \frac{k_i\ J_m'(k_ir_{i+1}) + D_{i,m}H_m^{(1)'}(k_i,r_{i+1})}{k_{i+1}J_m(k_ir_{i+1}) + D_{i,m}H_m^{(1)}(k_i,r_{i+1})}, \tag{S2}$$

where $D_{i,m} = \frac{b_{i,m}}{a_{i,m}}$. Using $D_{1,m} = 0$ and the continuities, the total scattering cross section can be obtained from:

$$C_s = \sum_m C_{s,m} = \sum_m \frac{2\pi}{\lambda}|D_{N+1,m}|^2, \tag{S3}$$

And the partial cross section will have a Lorenz line shape near the resonance wavelength:

$$C_{s,m} = \frac{4\gamma_m^2}{k_0[(k_0-k_m)^2+\gamma_m^2]}, \tag{S4}$$

from which k_m and γ_m (the damping rate) can be extracted, and resonance wavelengths with *Q*-factors can be obtained from $\lambda = 2\pi/k_m$ and $Q = k_m/2|\gamma_m|$.

References:

1 T. Kipp, H. Welsch, C. Strelow, C. Heyn and D. Heitmann, *Phys. Rev. Lett.*, 2006, **96**, 077403.

2 M. Hosoda and T. Shigaki, *Appl. Phys. Lett.*, 2007, **90**, 181107.

3 T. Zhan, C. Xu, F. Zhao, Z. Xiong, X. Hu, G. Huang, Y. Mei and J. Zi, *Appl. Phys. Lett.*, 2011, **99**, 211104.

4 F. Y. Zhao, T. R. Zhan, G. S. Huang, Y. F. Mei and X. H. Hu, *Lab Chip*, 2012, **12**, 3798-3802.

5 S. W. Tang, Y. F. Fang, Z. W. Liu, L. Zhou and Y. F. Mei, *Lab Chip*, 2016, **16**, 182-187.

6 P. Chýlek, *J. Opt. Soc. Am. B*, 1990, **7**, 1609-1613.

7 C. C. Lam, P. T. Leung and K. Young, *J. Opt. Soc. Am. B*, 1992, **9**, 1585-1592.

8 T. Reynolds, M. R. Henderson, A. François, N. Riesen, J. M. M. Hall, S. V. Afshar, S. J. Nicholls and T. M. Monro, *Opt. Express*, 2015, **23**, 17067-17076.